Polym. Bull. (2016) 73:2547–2555
DOI 10.1007/s00289-016-1684-5

ORIGINAL PAPER

Inverse opal photoelectrode of Nb-doped TiO_2 nanoparticles for dye-sensitized solar cell

Wonmok Lee[1] · Seulki Kim[1] · Jonghyeon Kang[2] · Kyusung Han[3] · Hyunjung Lee[2]

Received: 2 October 2015 / Revised: 1 April 2016 / Accepted: 19 April 2016 /
Published online: 23 April 2016

Abstract In this study, Nb-doped TiO_2 nanoparticles were prepared by solution synthesis, and utilized as photoelectrode for dye-sensitized solar cell aiming to obtain better photon-to-current conversion efficiency. Nb doping was carried out using two different Nb precursors, and subsequent hydrothermal treatment resulted in the size-controlled ($\sim$10 nm) Nb-doped TiO_2 nanoparticles with typical ellipsoidal shapes and anatase morphologies. It was observed that $NbCl_2$ precursor resulted in more uniform particle size, while Nb oxalate resulted in relatively broader particle size distributions and higher aspect ratio ellipsoid. Using these nanoparticles, 10 μm-thick porous inverse opal (IO) photoelectrodes were fabricated by coating the mixed aqueous dispersions of Nb-TiO_2 nanoparticles and polystyrene particles of 270 nm diameter on conductive glass followed by thermal sintering. DSSC single cell performance tests revealed that a photoelectrode from 2 mol% Nb- TiO_2 obtained from $NbCl_2$ exhibited 20 % enhancement for solar cell efficiency compared to bare TiO_2 IO.

Electronic supplementary material The online version of this article (doi:10.1007/s00289-016-1684-5) contains supplementary material, which is available to authorized users.

✉ Wonmok Lee
wonmoklee@sejong.ac.kr

✉ Hyunjung Lee
hyunjung@kookmin.ac.kr

[1] Department of Chemistry, Sejong University, 98 Gunja-Dong, Gwangjin-Gu, Seoul 143–747, Republic of Korea

[2] School of Advanced Materials Engineering, Kookmin University, 861-1 Jeongneung-Dong, Seoul, Republic of Korea

[3] Korea Institute of Ceramic Engineering and Technology, Icheon, Gyeonggi 467-843, Republic of Korea

Keywords Nb-doped TiO_2 nanoparticles · Sol-gel method · Raw material · Hydrothermal treatment · Inverse opal film · Photoelectrode · Dye-sensitized solar cell

Introduction

With increasing interest and demand for suitable electric power source for flexible and wearable devices, dye-sensitized solar cell (DSSC) has been one of the hottest research topics owing to the advantageous features such as light weight, flexibility, processing cost, etc. [1–4]. However, relatively low photon-to-current conversion efficiency (PCE) of DSSC is still an important challenge to be overcome. Many efforts have been devoted to improve PCE by engineering essential components of DSSC devices, such as electrolyte, dye, and photoelectrode. From materials point of view, titanium dioxide (TiO_2) nanoparticles are most frequently used as photoelectrode for DSSC due to their unique electronic bandgap and electron transporting ability. Recently, we reported a synthesis of TiO_2 nanoparticles which can be effectively applied to DSSC photoelectrode by wet coating [5, 6]. By doping Nb or W within TiO_2 lattices, it is reported that the optical and electronic properties can be further improved while preserving the original crystalline structure owing to similar ionic sizes of Nb and Ti [7–12]. The subsequent increase in electron-transport ability elevates current density, finally improving the efficiency of solar cell. In this study, we prepared the uniform sized Nb-doped TiO_2 nanoparticles, and inverse opal Nb-doped TiO_2 film was fabricated on FTO glass to be applied to the photoelectrode of dye-sensitized solar cell (DSSC).

Materials and methods

Synthesis of Nb-doped TiO_2 nanoparticles and PS μ-particle

Nb-doped TiO_2 nanoparticles were synthesized by three steps; sol-gel reaction–peptization–hydrothermal treatment. In results, small and uniform Nb-doped nanoparticles were obtained (see S-1). Spherical PS colloidal particles with 270 nm particle sizes were synthesized by a typical emulsion polymerization method using potassium persulfate (PPS, Aldrich) and sodium dodecylsulfate (SDS, Aldrich) as a radical initiator and a surfactant, respectively. Synthetic details are almost the same as described in the previous report [13].

Fabrication of Nb-TiO_2 IO photoelectrdoe and DSSC performance test

On a clean FTO glass (TEC-8, Pilkington), 7 % 1-butanol solution of Titanium(IV) bis(ethyl acetoacetato)-diisopropoxide solution (Aldrich) was spin coated, and the coated precursor film was thermally calcined at 450 °C to form a thin TiO_2 blocking layer. Using that as a bottom substrate, the PS/Nb-TiO_2 hybrid opal and subsequent Nb-TiO_2 IO photoelectrode were fabricated (see S-2 for detail). Using the Nb-TiO_2

IO photoelectrode, DSSC single cell was fabricated using the same procedures reported elsewhere [6] (see S-3 for detail). Photocurrent was measured using a source measuring unit (model 2400, Keithley) under AM 1.5G one sun condition. The data was compared with that of NREL-calibrated Si solar sell.

Characterization of nanoparticles and IO films

For characterization of nanoparticles and IO films, high resolution transmission electron microscopy (HR-TEM, tecnai F20, FEI), X-ray diffractometer (XRD, Rigaku D/Max-2500), and scanning electron microscopy (SEM, S-4700, HITACHI) were used. The reflective colors of the IO films were analyzed using (DSLR) camera (DSLR-A550, SONY).

Results and discussion

The prerequisites for TiO_2 nanoparticle to be utilized as an inverse opal structure are small particle size, uniform size distribution, high crystallinity and uniform shape. To achieve that, we employed a sequential synthetic method of sol-gel hydrolysis/condensation of Ti alcoxide, peptization, and hydrothermal treatment to obtain Nb-doped TiO_2 nanoparticle in a controlled manner (Fig. 1a, c). As shown in Fig. 1, a crude sol-gel reaction product of TiO_2 was mixed with peptization agent, to convert large irregular TiO_2 particles to very small and uniform nanoparticles with a few nanometer sizes, which are charge-stabilized due to the surface-adsorbed TMNOH molecules. Nb precursor was added during this stage, and Nb-doped TiO_2

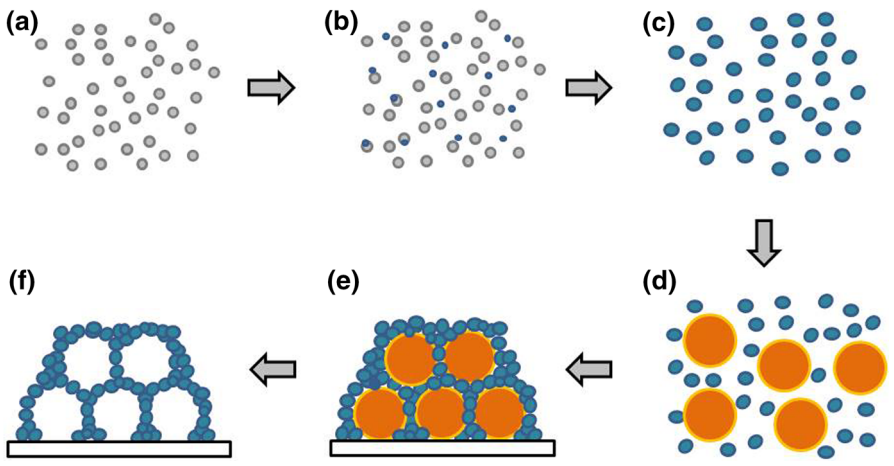

Fig. 1 Schematic representation of Nb-TiO_2 nanoparticle synthesis and IO fabrication. **a** TiO_2 particles by sol-gel reaction followed by peptization process, **b** mixing of Nb precursor and TiO_2 nanoparticles, **c** Nb-TiO_2 nanocrystals by hydrothermal reaction, **d** binary aqueous mixture of Nb-TiO_2 and PS particle, **e** binary opal film of ordered PS opal and Nb-TiO_2 on FTO by slide coating, **f** Nb-TiO_2 IO film after thermal calcinations

nanoparticle could be obtained. After peptization, the translucent dispersions were transferred to a bomb reactor to undergo overnight hydrothermal reaction. The final products were milk-like aqueous dispersions of Nb-doped TiO_2 nanocrystals, and directly used for slide coating with PS particles. The atomic % of Nb of the resulting nanoparticles was analyzed by EDX. In this study, the effect of Nb doping ratio on the crystalline morphology of TiO_2 nanoparticle was investigated. In repeated attempts, mixing of more than 2 mol% of $NbCl_2$ precursor with TiO_2 sol resulted in a serious coagulation of TiO_2 nanoparticles due to high acidity of $NbCl_2$. Nonetheless, 2 mol% of Nb doping on TiO_2 was successfully carried out using $NbCl_2$, and Nb-doped TiO_2 nanoparticles with small particle size (8.1 nm) could be obtained. When NbOXL was used as Nb precursor, there was no significant coagulation problem, and four Nb-doped TiO_2 nanoparticles with different doping ratio (1, 2, 4, and 6 mol%) could be obtained. However, the more Nb doping was attempted, the larger particle size and higher aspect ratio ellipsoidal shape was resulted. HR-TEM analysis revealed Nb-doped TiO_2 nanoparticles from different Nb precursors show non-spherically shaped Nb-TiO_2 nanocrystals [6] (see S-4 for detail). The particle sizes and crystallinities of the Nb-doped TiO_2 nanoparticles were also characterized by XRD as shown in Fig. 2.

Through powder XRD analysis as shown in Fig. 2a, it was found that bare TiO_2 and Nb-doped TiO_2 nanocrystals from two different Nb precursors exhibited anatase crystalline phases. For the calculation of the average particle sizes, Scherrer analysis was applied to both [101], [200] peaks of anatase TiO_2 which appeared at 25.1° and 47.1°, respectively, and the average particle sizes are summarized in Table 1. As shown in Fig. 2a, ~0.5° shift of the [101] peak from NbOXL-doped TiO_2 evidently tells us the increased crystalline lattice size due to the inclusion of Nb oxide within TiO_2. However, Nb-TiO_2 from $NbCl_2$ exhibited very noisy signals to judge the peak shift due to the smallest particle size among all.

As shown in Fig. 2b, the characteristic diffraction peaks of Nb-TiO_2 nanoparticles generally become narrower as Nb doping ratio increases. In results, the calculated particle size increased with doping ratio. It should be noted that we

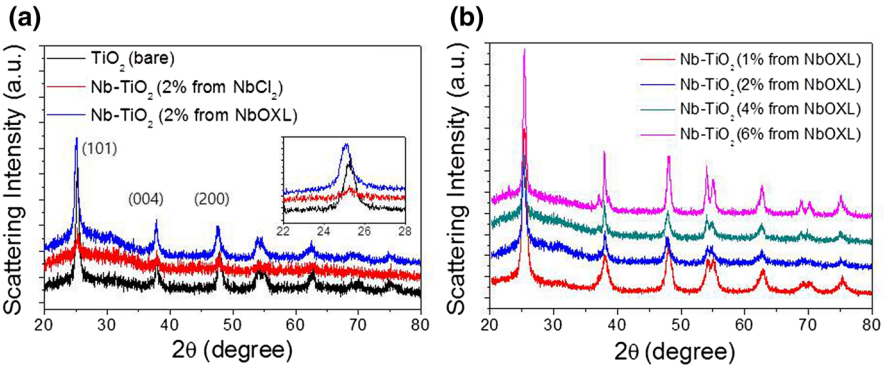

Fig. 2 XRD patterns of TiO_2 with or without Nb doping. **a** Depending on Nb precursor (*inset* enlarged graph) **b** depending on doped ratio from 1 to 6 mol%

assumed the spherical particle shape for Scherrer analysis, which is not true for our nanoparticles, thus the calculated particle sizes just show a general trend [14].

Since the six different nanoparticles were well stabilized in water without significant sedimentation, they formed uniform binary mixtures with PS μ-particle. The respective binary mixtures could be uniformly coated on FTO glass using a slide coating apparatus as shown in Fig. 3a. With a slow retreat of top cell, the exposed Nb-TiO_2 and PS dispersion formed a uniform wet film, and hot air blown on top of the film expedited self-assembly of binary opal film as schematically demonstrated in Fig. 3b. As shown in Fig. 3c, the binary opal film exhibited reddish brown color which changed into a shiny blue IO film upon thermal calcinations to remove PS opal template. The photographs shown in Fig. 3c were taken from the hybrid opal film of PS/Nb-TiO_2 and the subsequent Nb-TiO_2 IO film where 2 % Nb-TiO_2 from $NbCl_2$ was used. The reflective color of IO film shown in Fig. 3c comes from a highly ordered IO structure to diffract visible light, which is evidently shown

Table 1 Average particle sizes of Nb-doped TiO_2 nanoparticles characterized by XRD

Sample	Bare TiO_2	Nb 2 % ($NbCl_2$)	Nb 1 % (NbOXL)	Nb 2 % (NbOXL)	Nb 4 % (NbOXL)	Nb 6 % (NbOXL)
Size (nm)	9.5 ± 0.6	8.1 ± 1.4	11.2 ± 1.9	9.9 ± 0.1	16.1 ± 4.0	15.3 ± 0.9

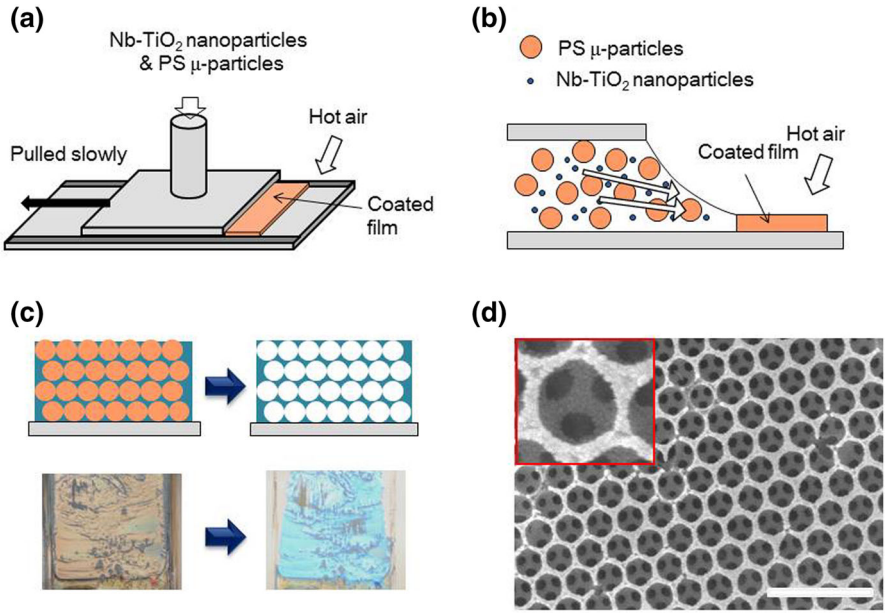

Fig. 3 Schematic of **a** slide coating apparatus, **b** hot air aided coating of binary opal film, **c** Nb-TiO_2 IO film formation by thermal calcination, **d** SEM images of the Nb-TiO_2 IO film using $NbCl_2$ with 2 mol% of Nb doping. *Inset* shows a magnified view of the same sample. *Scale bar* indicates 1 μm

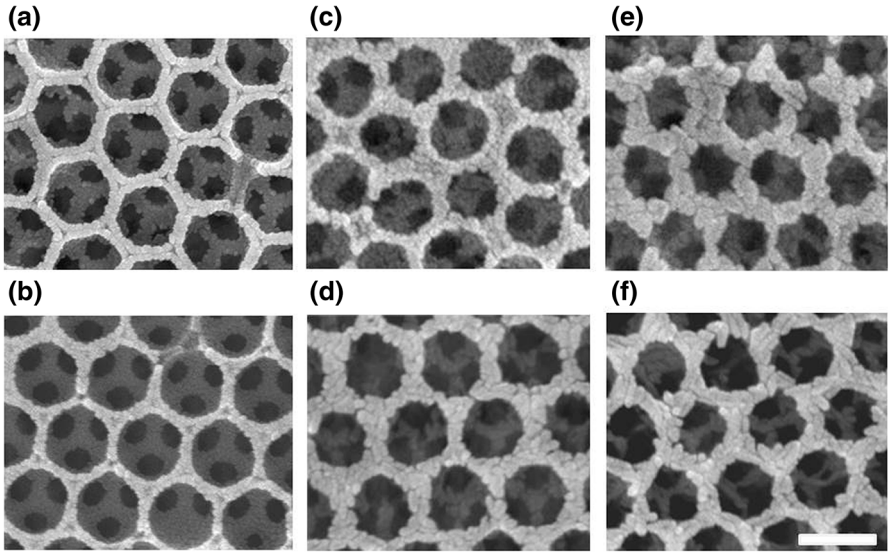

Fig. 4 SEM images of the IO films of **a** bare TiO_2, **b** 2 % Nb-TiO_2 using $NbCl_2$, **c** 1 %, **d** 2 %, **e** 4 %, **f** 6 % Nb-TiO_2 using NbOXL. Six images are at the same magnification. *Scale bar* indicates 300 nm

in Fig. 3d which is a SEM image of the Nb-TiO_2 IO film [6]. In the inset image, we can distinguish small and uniform Nb-TiO_2 nanoparticles forming IO scaffold.

In Fig. 4, the IO structures made from six Nb-TiO_2 samples are shown. Each IO film was templated by the same PS μ-particle. Since the synthetic condition for every nanoparticle was the same only except the addition of different amount Nb sources, the pore sizes of six IO samples were practically the same, and thus one can easily compare the particle sizes and shapes of respective Nb-TiO_2 nanoparticles in Fig. 4. In addition, all the IO film thicknesses were also similar to be ~10 μm (see S-6 for detail). It is evidently shown that the shapes of Nb-TiO_2 particles prepared from NbOXL are irregular than those of bare TiO_2 or $NbCl_2$, and higher Nb contents resulted in not only larger particle size but also higher aspect ratio of the ellipsoidal shape. The apparent particle sizes shown in Fig. 4 appear to be larger than the values in Table 1. Since the particle size generally increases by thermal sintering, those observations are reasonable.

Using the IO films on FTO as the respective photoelectrodes, DSSC single cells were fabricated as schematically shown in Fig. 5a, and the solar cell performance were measured as shown in Fig. 5b. The solar cell performance results are also summarized in Table 2.

It was found that 2 % Nb-TiO_2 IO photoelectrode from $NbCl_2$ precursor shows ~20 % enhancement of DSSC performance compared to that with undoped TiO_2 IO, while IO films of Nb-TiO_2 from NbOXL showed lower power performances. Judging from the significantly high J_{SC} of Nb-TiO_2 from $NbCl_2$, the reason for the enhanced efficiency can be attributed to an improved electron mobility of Nb-doped TiO_2 photoelectrode to facilitate electron transport through the IO film which could

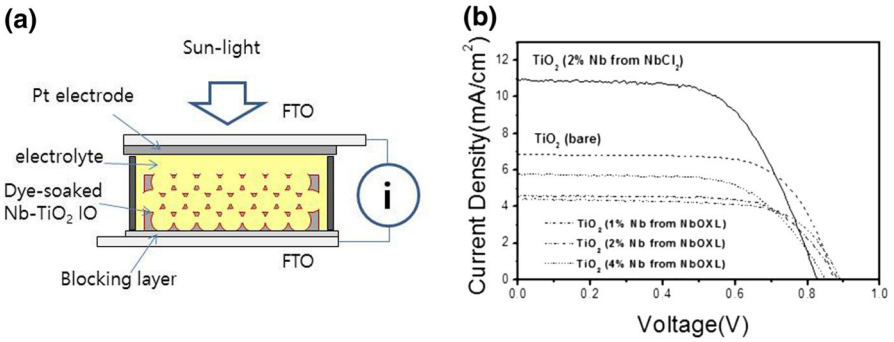

Fig. 5 **a** Schematic representation of DSSC single cell showing a dye-soaked Nb-TiO_2 IO photoelectrode, **b** IV curves measured from the single cells containing various Nb-TiO_2 photoelectrodes

Table 2 DSSC single cell performances with Nb-doped TiO_2 as photoelectrode

Source of photoelectrode (Nb mol%)	Active area (cm^2)	J_{sc} (mA/cm^2)	Voc (V)	FF (%)	CE (η) (%)
Bare TiO_2	0.367	6.85	0.87	69.6	4.16
Nb-TiO_2 from $NbCl_2$ (2 %)	0.356	11.14	0.83	56.8	5.25
Nb-TiO_2 from NbOXL (1 %)	0.305	4.65	0.89	62.5	2.59
Nb-TiO_2 from NbOXL (2 %)	0.322	4.38	0.89	66.6	2.61
Nb-TiO_2 from NbOXL (4 %)	0.340	5.87	0.86	58.4	2.94

affect higher photocurrent generation in the DSSC single cell [15]. However, every Nb-TiO_2 photoelectrode from NbOXL exhibited small J_{SC} even compared to bare TiO_2. Besides the doping effect, the mechanical integrity of IO structure is important [16]. As shown in Fig. 5, the irregularly shaped nanoparticles should have deteriorated the formation of electron pass which should be assured between the nanoparticles' junction. Moreover, such particles could not fill the interstitial spaces of PS opal due to nonspherical shape. As an evidence, hybrid opal films of PS/Nb-TiO_2 from NbOXL and the corresponding IO film exhibited blue-shifted reflection colors compared to those from $NbCl_2$ which imply overall refractive indices are smaller (see S-7). Poor filling factor and mechanical strength was most serious for the IO films from NbOXL 6 %, which in fact was highly fragile, and therefore, we couldn't obtain a reasonable single cell performance using it as photoelectrode. In this regard, we could conclude that not only high doping of Nb but also the particle size and morphology affect the efficiency of DSSC device.

Conclusion

Via sol-gel synthesis followed by subsequent peptization and hydrothermal treatment, we successfully synthesized Nb-doped TiO_2 nanoparticles using two different Nb sources, with doping rates up to 6 mol%. The size of nanoparticles

ranging from 8 to 16 nm and anatase crystalline phase was characterized by XRD. The binary aqueous dispersions of Nb-TiO_2 nanoparticles and PS μ-spheres successfully formed highly ordered PS/Nb-TiO_2 opal films on FTO glass. Subsequent thermal sintering resulted in shiny blue IO films of Nb-TiO_2 with various doping ratios, which could be directly used as photoelectrodes for DSSC. DSSC single cell performance tests revealed that a single cell with 2 % Nb-TiO_2 IO photoelectrode from $NbCl_2$ precursor shows $\sim$20 % enhancement of DSSC performance compared to that with bare TiO_2 IO, while IO films of Nb-TiO_2 from NbOXL showed lower power performances due to poor mechanical integrity of IO structures originating from irregular particle shapes.

Acknowledgments This study was financially supported by Basic Science Research Program through the National Research Foundation of Korea (NRF) funded by the Ministry of Education, Science and Technology (2013R1A1A2011168), and partially supported by Civil Military Technology Cooperation Center (CMTC) (15-CM-EN-08).

References

1. Gratzel M (2005) Dye-sensitized solid-state heterojunction solar cells. MRS Bull 30:23–27
2. Morton O (2006) Solar energy: a new day dawning? Silicon valley sunrise. Nature 443:19–22
3. Mihi A, Calvo ME, Anta JA, Miguez H (2008) Spectral response of opal-based dye-sensitized solar cells. J Phys Chem C 112:13–17
4. Kwak ES, Lee W, Park NG, Kim J, Lee H (2009) Compact inverse-opal electrode using non-aggregated TiO_2 nanoparticles for dye-sensitized solar cells. Adv Func Mater 19:1093–1099
5. Seo YG, Lee H, Kim K, Lee W (2010) Transparent thin films of anatase titania nanoparticles with high refractive indices prepared by wet coating process. Mol Cryst Liq Cryst 520:201–208
6. Seo YG, Woo J, Lee H, Lee W (2011) Rapid fabrication of an inverse opal TiO_2 photoelectrode for DSSC using a binary mixture of TiO_2 nanoparticles and polymer microspheres. Adv Funct Mater 21:3094–3103
7. Miyagi T, Kamei M, Sakaguchi I, Mitsuhashi T, Yamazaki A (2004) Photocatalytic property and deep levels of Nb-doped anatase TiO_2 film grown by metalorganic chemical vapor depostion. Jpn J Appl Phys 1(43):775–776
8. Su H, Huang Y, Chang Y, Zhai P, Hau NY, Cheung PCH, Yeh W, Wei T, Feng S (2015) The synthesis of Nb-doped TiO2 nanoparticles for improved-performance dye-sensitized solar cells. Electrochim Acta 182:230–237
9. Quan LN, Jang YH, Jang YJ, Kim J, Lee W, Moon JH, Kim DH (2015) Mesoporous carbon-TiO2 beads with nanotextured surfaces as photoanodes in dye-sensitized solar cells. Chem Sus Chem 7:2590–2596
10. Horie Y, Watanabe T, Deguchi M, Asakura D, Nomiyama T (2013) Enhancement of carrier mobility by electrospun nanofibers of Nb-doped TiO_2 in dye-sensitized solar cells. Electrochim Acta 105:394–402
11. Chun JH, Kim JS (2014) Comparison of different structures of niobium oxide blocking layer for dye-sensitized solar cells. J Nanosci Nanotech 14:6226–6230
12. Lim SH, Park KW, Jin MH, Ahn S, Song J, Hong J (2015) Facile preparation of a Nb_2O_5 blocking layer for dye-sensitized solar cells. J Electroceramics 34:221–227
13. Kim S, Seo YG, Cho Y, Shin J, Gil SC, Lee W (2010) Optimization of emulsion polymerization for submicron-sized polymer colloids towards tunable synthetic opals. Bull Kor Chem Soc 31:1891–1896

14. Lee W, Kim I, Ok I, Ahn D, Lee H, Kim JH, Kim K (2014) Solution processed thin films of Nb-doped TiO_2 nanoparticles as hole blocking layer for organic solar cells. Thin Solid Films 553:161–165
15. Kubacka A, Colon G, Fernandez-Garcia M (2009) Cationic (V, Mo, Nb, W) doping of TiO_2-anatase: a real alternative for visible light-driven photocatalysts. Catal Today 143:286–292
16. Das P, Sengupta D, Kasinadhuni U, Mondal B, Mukherjee K (2015) Nano-crystalline thin and nano-particulate thick TiO_2 layer: cost effective sequential deposition and study on dye-sensitized solar cell characteristics. Mater Res Bull 66:32–38